Acta Geotechnica (2024) 19:3283–3298
https://doi.org/10.1007/s11440-024-02261-8

RESEARCH PAPER

Hydraulic breakthrough of clay smears due to technical and natural actions

Gerd Gudehus[1] · Christian Karcher[2]

Published online: 25 April 2024

Abstract
We outlined earlier in this journal by means of finite element simulations how patterns of normal faults arise by a synsedimentary tectonic extension, and how clay smears evolve therein. In the present paper, we show how hydraulic breakthroughs of clay smears can arise so that water, gas and mud rise in faults. Mechanical properties of sand and clay are introduced first for the stable range and then for rupture and internal erosion. Our numerical simulations for the evolution of normal faults and clay smears are discussed in light of critical phenomena. Water assembled in an open-cast mine about 20 years ago as the critical hydraulic gradient in a clay smear dropped to the actual one due to the rapid excavation-induced deformation. The latter led to a critical point under an excavation the slope of which was parallel to a nearby normal fault. Clay smears can also break by earthquakes so that the critical hydraulic gradient drops to the actual one caused by methane with an excess pressure. This can lead to hydraulic breakthroughs and cold eruptions at outcrops of faults.

Keywords Clay smears · Fault · Hydraulic gradients · Tectonics

1 Introduction

About 20 years ago warm turbid water accumulated in the deepest part of a lignite mine west of Cologne/Germany [25]. The influx from below was reduced by pumping water out of deep wells and came to an end after some days. Causative mechanisms were clarified in a joint effort of three universities so that events could be avoided ever since. This investigation led to a publication on normal faults and clay smears [5], while the present paper needed more time as critical phenomena with geo-matter were considered more explicitly, and as the rate-dependence of clay had to be taken into account.

Neugebauer questions constitutive relations with representative spatial averages for complex earth systems because of scale effects [21]. Mean-field theories work with stress–strain relations of so-called simple materials without scale effects, in particular for geo-materials. However, geo-matter is not a simple material as its spatial and temporal distributions of mechanical quantities are not smooth so that gradients and rates are not properly justified. Hypoplastic and visco-hypoplastic relations, employed in our earlier paper and again in the present one, are of limited validity as they refer to lab tests with reconstituted samples, i.e. with geo-material instead of geo-matter (Sect. 2). The difference is due to rather fractal patterns of shear bands and cracks which change by critical phenomena and leave back structural traces. Therefore, the derivatives related by Darcy's law are likewise not properly justified. As without fractality, the solid mineral is neutral with respect to changes of pore water pressure (principle of effective stress), while fabrics of hard grains exhibit rate-independence, the response of clay fabrics to slow deformations is visco-plastic (ductile) and to rapid ones it is cataclastic (brittle).

Darwin [2]—second son of Charles Darwin, astronomer and mathematician—observed that dense dry sand in a box led to an active limit state by means of a yielding wall, dilates first quasi-statically in a Coulomb shear zone and

✉ Gerd Gudehus
gerd.gudehus@kit.edu

Christian Karcher
christian.karcher@rwe.com

[1] Institute of Soil and Rock Mechanics, Germany, Engler Bunte Ring 14, 76131 Karlsruhe, Germany

[2] Geotechnical Department, RWE Power AG, Zum Gut Bohlendorf, 66399 Bergheim, Germany

contracts suddenly thereafter with a hissing noise. Lempp [16] observed nearly the same behavior with water-saturated sandstone in triaxial tests: first a quasi-static dilation in evolving shear bands and/or cracks, then a contractant collapse with grain crushing and rise of pore pressure. More generally speaking, it appears that patterns of shear bands and cracks evolve alongside with slow actions up to a kind of percolation and a seismogenic chain reaction [8]. Our simulated slow evolutions of normal faults and clay smears [5] are reconsidered as quasi-static critical phenomena in Sect. 3. As always in structural geology, however, initial and boundary conditions cannot be understood like with mean-field theories because of the ever-present fractality.

The internal erosion of geo-matter is localized to channels so that mean-field approaches are evidently inadequate. This is outlined in Sect. 4 by means of sand samples with embedded clay bands. An erosive breakthrough is achieved if the hydraulic gradient reaches a critical amount. The latter is reduced by a localized dilation of clay, while critical gradients grow again if openings are closed by subsequent shearing. For explaining the event in an open-cast mine mentioned above deformations due to the excavation are estimated by means of finite element simulations (Sect. 5). As the deformation of clay smears is reversed, more focussed and more rapid than during the tectonic evolution before it can lead to a localized dilation so that the critical hydraulic gradient drops down to the actual gradient. This occurred under the corner of an excavation with a cut slope nearly parallel to a nearby normal fault.

While such events can be avoided by a suitable orientation of cut slopes they are inevitable in formations with natural methane accumulations under excess pressure in the case of strong seismic activity (Sect. 6). Again the hydraulic gradient in a clay smear can get critical after a localized dilation due to a rapid deformation, but the complexity of clay seals and of rapid tectonic deformations eludes a more detailed analysis. We conclude that the hydraulic breakthrough of clay smears can lead to an eruption of water, gas and mud, and that some features of such critical phenomena can be identified (Sect. 7). Thus the present paper may serve as an inductive addendum to the recent overview on clay smears by Vrolijk [26], whereas a rather deductive explanation of critical phenomena with geo-matter is yet out of reach.

2 Constitutive relations

Sand and gravel are captured for our finite element simulations by a *hypoplastic* relation [4, 14]. Therein the effective stress rate is a tensor function of strain rate, stress and void ratio, i.e. $\dot{\sigma}'_{ij} = f_{ij}(\dot{\epsilon}_{ij}, \sigma'_{ij}, e)$. With water saturation the effective—or solid fabric—stress σ'_{ij} does not depend on the pore water pressure p_w, i.e. $\sigma'_{ij} = \sigma_{ij} - p_w\delta_{ij}$ holds with total stress σ_{ij}. The response $\dot{\sigma}'_{ij}$ is synchronous to the drive $\dot{\epsilon}_{ij}$, which is called rate-indepedence and means $f_{ij}(\lambda\dot{\epsilon}_{ij}) = \lambda f_{ij}(\dot{\epsilon}_{ij})$ for any $\lambda > 0$. The response is nonlinear, i.e. $f_{ij}(-\dot{\epsilon}_{ij}) \neq -f_{ij}(\dot{\epsilon}_{ij})$ holds except for a narrow elastic range. So-called critical states enable stationary shearing, then σ'_{ij} satisfies a Coulomb condition and is aligned by an isochoric $\dot{\epsilon}_{ij}$ (i.e. with $\dot{\epsilon}_{ii} = 0$), and the void ratio e_c is lower for a higher fabric pressure $p' \equiv \frac{1}{3}\sigma'_{ii}$. Isobaric deformations, i.e. strain rates with constant p', are contractant ($\dot{e} < 0$) or dilatant ($\dot{e} > 0$) if the ratio τ/p' of directionally averaged shear stress τ and fabric pressure p' is below or above $\tan\varphi_c$, respectively, with an e-and p'-independent critical friction angle φ_c.

A hypoplastic relation requires three parameters for monotonous deformations: φ_c, a granulate hardness h_s for the p'-dependence of e_c, and the critical void ratio e_{c0} for $p' = 0$. Four further parameters are nearly the same for different granular sediments. Triaxial tests are used for validating the proposed relation and for calibrating its parameters. For the simulations in the present paper, they were carried out with sand and gravel from boreholes west of Cologne with fabric pressures up to 10 MPa. Reconstituted samples from boreholes can represent natural formations of sand and gravel for the stable range with $\tau/p' \leq \tan\varphi_c$ in spite of spatial fluctuations of grain size d_g, void ratio e and fabric stress σ'_{ij}.

Denser than critical grain fabrics ($e \leq e_c$) exhibit *dilation* localized in shear bands with constant p' when they are sheared in the instable range with $\tau/p' > \tan\varphi_c$ [4]. A single shear band appears at samples in biaxial tests, its inclination against the direction of the biggest principal fabric stress σ'_1 comes close to $\pi/4 - \varphi_c/2$. The latter suits to the contact of a Coulomb tangent to Mohr's circle, and is similarly obtained by means of a quasi-static bifurcation from biaxial shortening to shearing. A similarly inclined shear band can be obtained with finite elements and a hypoplastic relation, but then its thickness equals the arbitrary element size. The observed thickness of about ten grains cannot be explained with a constitutive relation of σ'_{ij} and ϵ_{ij}. Thus a grain fabric in the instable range is no more a simple material without a characteristic length.

The rather heuristic hypoplastic relation is justified by means of specific elastic and seismic *energies* w_e and w_s, respectively, for the stable range [6, 10]. w_e, depending on e and elastic strain invariants of the grain fabric, is the potential of fabric stress at rest in such a way that it has a saddle point at the Coulomb limit $\tau/p' = \tan\varphi_c$ (Fig. 1). In the stable range with $\tau/p' \leq \tan\varphi_c$ this w_e is convex with

respect to the elastic strain components. In this range redistributions of the grain fabric and its elastic strain are activated by a heat-like micro-seismicity (audible as a crackling noise) although its energy w_s per unit of fabric volume is far smaller than w_e. w_s is fed by the imposed strain rate and turns into heat with a relaxation time far shorter than the deformation time, therefore the response is almost synchronous or rate-independent as observed and assumed with hypoplastic relations.

A shear band thickness of ca. $10d_g$ is obtained by means of additional *polar quantities*, viz. inter-granular rotations and resisting moments. The extended constitutive relation implies the grain size d_g as a characteristic length. Combined with a minute initial fluctation of e, this extension leads to a rather fractal pattern of shear bands which was similarly observed with X-rays in biaxial tests [4]. A similar pattern was obtained by the extension of a granular layer upon a rigid smooth base, Fig. 2. It does not depend on the arbitrary length of the layer as distributions at the right-hand lateral boundary are the mirror-image of the ones at the left-hand boundary. The lateral extension leads first to a few shear bands with a distance of about half the layer thickness, and to less marked narrower bands between them with the same inclination. With a continued extension the bands do net get flatter, while secondary bands get more marked near the base, and offsets arise at the free surface. A quasi-static extension beyond ca. 20% is numerically impossible.

Evolutions like in Fig. 2 constitute a *critical phenomenon* which cannot be captured with constitutive relations of stress and strain rates as the ones indicated above for the stable range. As with thermodynamic critical phenomena the free energy is no more convex (cf. Fig. 1), but differently from gases and liquids arising polar quantities enable a quasi-static continuation. More precisely speaking, rearrangements are activated alongside with an imposed deformation by an incoherent micro-seismicity beyond the stable range without polar quantities. The

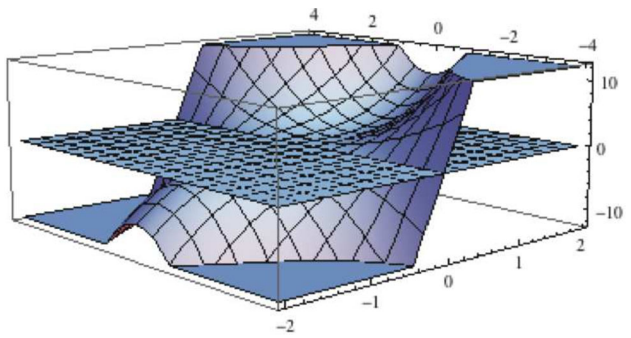

Fig. 1 Specific elastic energy w_e (− 10 to 10) versus first (− 4 to + 4) and second invariant (− 2 to + 2) of elastic strain of a grain fabric; blown-up local deviations from the tangential plane at a critical point

formation of rather *fractal* patterns, visible e.g. in Fig. 2 by secondary shear bands between primary ones, differs from the one in gas or liquid at a critical point by a uniform inclination with respect to a major principal stress, and by its permanence if the imposed deformation is stopped. As void ratio, stress and rearrangement are no more smoothly distributed constitutive relations of simple materials get invalid. The inclination of shear bands versus the direction of the major principal stress is but roughly determined by its direction as this kind of force-density gets questionable with fractal fluctuations. More generally speaking, at critical points geo-material turns into geo-matter for which relations of spatial averages are insufficient.

A quasi-static shear-banding cannot be continued when the elastic energy including polar quantities reaches again a critical point. The ensued *contractant collapse* of the grain fabric due to buckling force chains is seismogenic because of the uniform alignment by the spatially averaged principal stress [8]. This is confirmed by Darwin's [2] observation with dense fine dry sand in a box with a yielding wall: after a quasi-static dilation in a Coulomb zone a contractant collapse causes a hissing noise. Darwin states that 'this breakdown of equilibrium eludes mathematical treatment' due to traces of placement. This holds true until present as grain fabrics exhibit a spatio-temporally changing random fractality, all the more as the pore pressure of water-saturated grain fabrics rises with a collapse which enhances seismogenic chain reactions. As concluded similarly from triaxial tests with water-saturated sandstone by Lempp [16], thus grain fabrics exhibit two kinds of critical phenomena: dilatant quasi-static ones with evolution of fractal patterns, and contractant kinetic ones of a more chaotic kind. The present paper focusses on successions of both, including an internal erosion starting at clay smears, so we turn now to clay.

Clay consists of mineral particles with lower activation energies of molecular dislocations than for contact islands of hard grains [24]. Therefore it exhibits rate-dependence (e.g. Fig. 3a), creep and relaxation, which was captured by a *visco-hypoplastic* relation [4, 22] for our numerical simulations. Therein the dilation by shearing with constant fabric pressure p' and the contraction just after its reversal, depend not only on p' and void ratio e, but also on the amount of strain rate $\dot{\epsilon}$. The compression under constant p' is bigger than with hard grains, more delayed as the permeability is lower, and enhanced by volumetric creep. The critical void ratio e_c attained by continued shearing is more reduced by a higher p' than with sand, and increases markedly if $\dot{\epsilon}$ rises by several orders of magnitude. A visco-hypoplastic relation requires four parameters: a critical friction angle $\tan\varphi_c$, a compression index λ, a critical void ratio e_{cr} for $p' = p_r$ (like in the Cam Clay model), and a

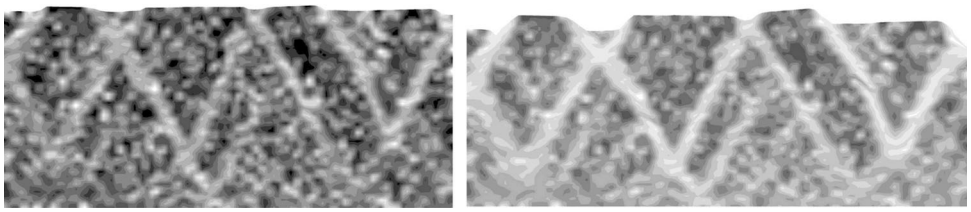

Fig. 2 Simulated extension of an initially 10 cm long sand layer with ca. 1 mm grain size and polar quantities. State at the right boundary as at the left one with reflected orientation, configurations after 10% (left) and 20% extension (right), black zones dense, white bands dilated [4, 23]

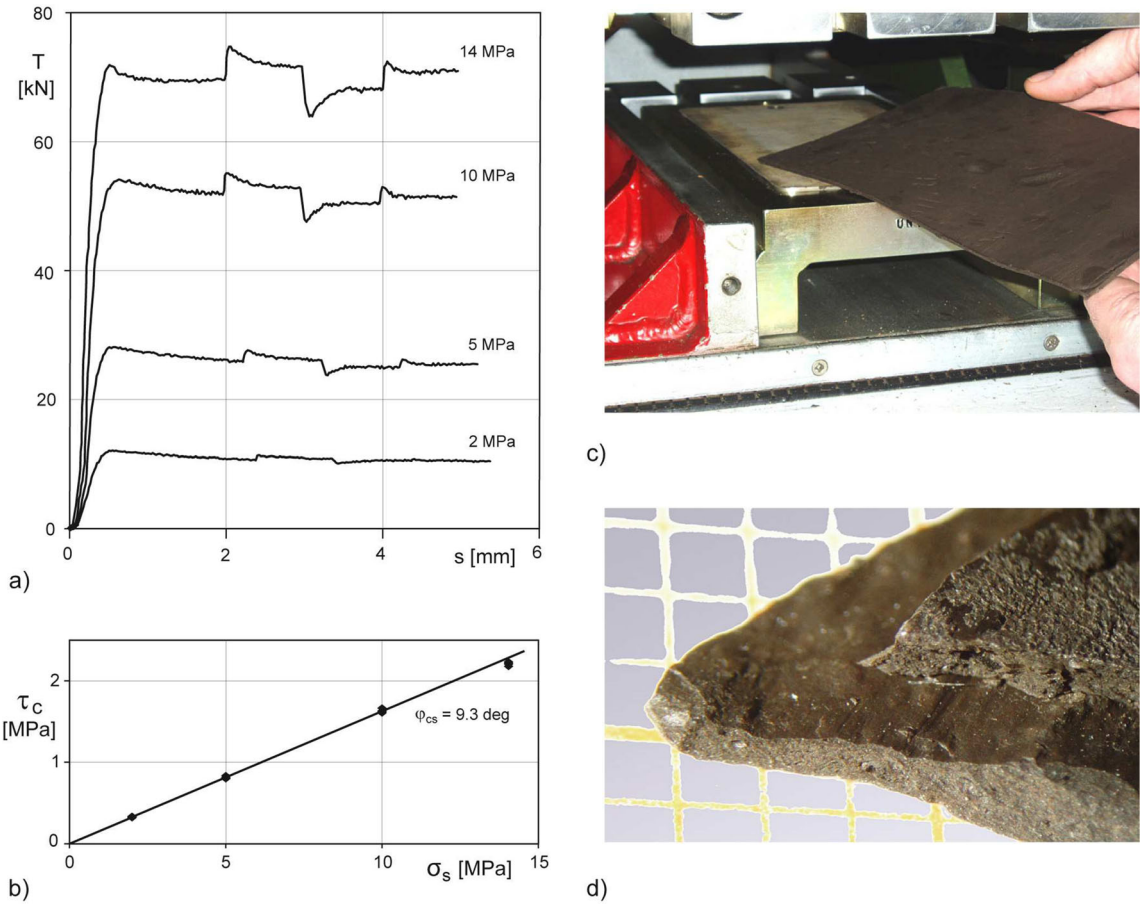

Fig. 3 Thin layer shear tests with clay from an open-cast mine in the Lower Rhenish basin: **a** response to shearing with rates suddenly increased by factor 10 and reduced by factor 100 under different pressures, **b** shearing resistance versus pressure (except just after a sudden change of shear rate), **c** placing a pre-compressed clay disc with suction upon a filter plate (movable loading plate lifted), **d** shear band after an experiment (square width 1 mm) [1]

viscosity index I_v (which equals the inverse of the exponent in Norton's law for stationary creep).

The *localized dilation* of clay at the verge of stability depends thus not only on effective stress and void ratio, but also on the amount of overall strain rate $\dot{\epsilon}$. Shear bands with $e = e_c$ are very thin and clay particles are aligned therein (e.g. Fig. 3d). Patterns of them evolve with imposed deformations after a pre-compression (e.g. Fig. 4) and/or if $\dot{\epsilon}$ is far bigger than before. Dilating bands can take up pore water from the neighbored fabric without overall seepage [4]. Fast deformations can lead to a cavitation of pore water into vapor, followed by a capillary entry of gas if present in the surroundings, so that cracks arise. A rupture occurs with delay after imposing and maintaining a higher than critical shear stress for the initial e and p' as the dilation towards e_c for the overall p' is impeded by a lower than hydrostatic pore water pressure p_w [1], which in turn can lead to cracks.

The formation of fractal shear bands and cracks in clay can occur quasi-statically as reaction to an imposed

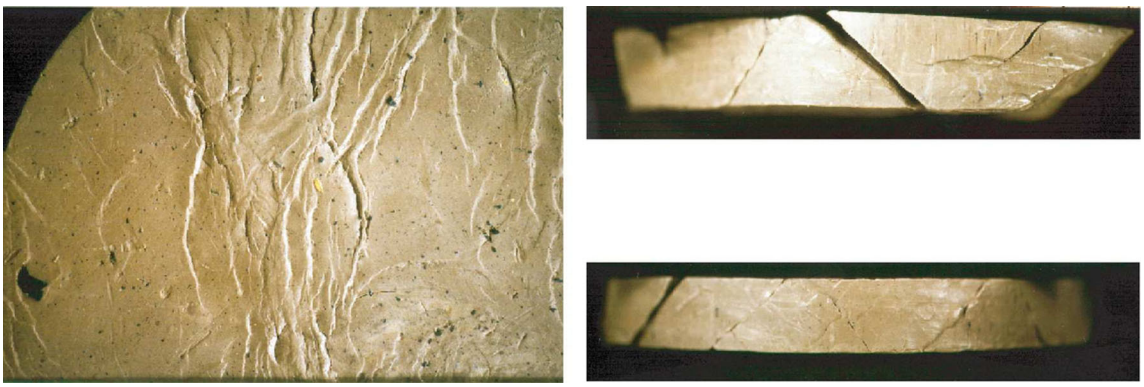

Fig. 4 Clay disc after squeezing between smooth plates with grease and rubber membranes. Horizontal surface without membrane (left), lateral surface with shear bands; opened ones were closed by pressure in subsequent tests (right) [28]

deformation, but differently from sand it is rate-dependent due to thermally activated dislocations at particle contacts and because of seepage from a contracted vicinity. Calculations with visco-hypoplastic relations can at best indicate the onset of such *critical phenomena*, but not their evolution because with this kind of geo-matter stress and strain as spatial averages get again insufficient for constitutive relations. Experiments do not indicate a contractant seismogenic collapse like with sand or sandstone, which may be attributed to viscous damping and low permeability of the clay fabric. We leave aside the softening of fault gauge by self-heating with high strain rates as clay smears take part in rather slow overall deformations.

3 Internal erosion

An *internal erosion* of fine particles occurs if these are not sufficiently supported against seepage forces by an adjacent grain fabric. For judging erosive breakthroughs of clay smears, about 1.5 cm thick slices of clay were placed horizontally in cylindrical samples of sand or gravel with 10 cm diameter, and exposed to an increasing hydraulic gradient up to a breakthrough in oedometer and triaxial setups [28]. Remoulded clay samples from a lignite mine west of Cologne were consolidated under the former overburden pressure. Before placing in the oedometer some clay discs were squeezed between smooth plates so that they had shear bands (Fig. 4). Other clay discs were squeezed similarly by axial loading in the triaxial setup before imposing hydraulic gradients. Critical values of the latter, recognized from sudden seepage and confirmed by erosion holes, are represented in Fig. 5. They suit to values calculated by means of limit equilibria of clay in a shear band, bridging a gap between adjacent grains with an effective cohesion adapted to the previous consolidation.

Critical gradients are somewhat bigger with reconstituted samples than with undisturbed ones (cf. black and white points near the lower curve of Fig. 5) as the latter have cracks which are not completely closed by re-compression. The internal erosion is evidently enhanced by wider pore sizes of adjacent formations, lower pressures, shear bands or cracks in the clay fabric and an increase of the osmotic repulsion of fine particles. The critical gradients observed in the oedometer exhibit a wider scatter than with the triaxial device, and are about ten times bigger without shear bands. Pore channels widened by an on-going erosion can be closed if the remaining fabric of clay particles shifts aside. However, such a closure requires a kinematic freedom which was not given in Zou's [28] experiments.

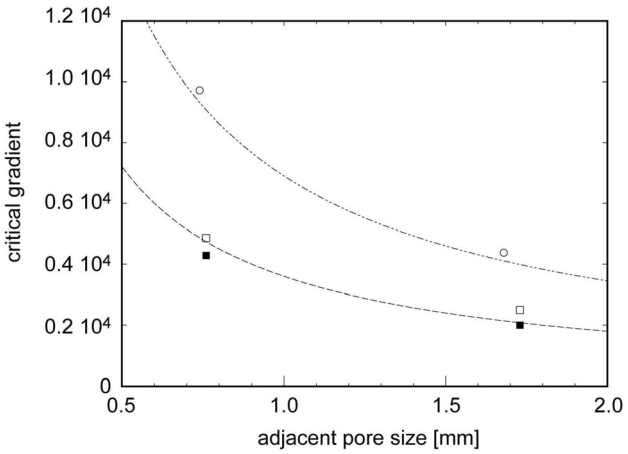

Fig. 5 Critical hydraulic gradients of clay discs with shear bands versus pore size of a neighbored grain fabric, observed in a triaxial setup (points) and calculated (neighbored curves). Lower values with 0.4 MPa confining pressure, upper ones with 0.8 MPa; clay from a mining pit, undisturbed (black points) or remoulded (white points) [28]

In addition, a reconstituted inclined clay disc was placed in a bigger triaxial setup between gravel in a sample of 0.8 m diameter, and sheared by an increasing axial force with a constant confining pressure (Fig. 6). Differently from the

experiments by Zou [28], an observable seepage was not achieved with hydraulic gradients up to 7000, and higher ones where the clay disc was thinned by shearing. The dismantled clay disc had an erosion hole which was not going through. This indicates a *self-healing* of the slightly eroded clay disc by continued shearing, which could not occur in Zou's experiments. In the latter the clay got cracks after compression with a higher pressure than after embedding it in sand or gravel, whereas it was hardly dilated in shear bands during the big-size triaxial test with a rather slow overall deformation.

Enhanced by shear bands or cracks, the internal erosion is a *critical phenomenon* which evidently eludes mathematical treatment with a mean-field theory (cf. [11]). Critical hydraulic gradients for the onset of such chain reactions at the contact of clay and sand can reach almost 10^4 after remoulding and consolidation of clay with pressures of up to 5 MPa, while they can drop to about 10^3 with shear bands or cracks, respectively, and can grow again by a subsequent slow shearing. An erosion channel can evolve in an adjacent granular formation as its critical gradients for an onset of internal erosion can be lower than 10 due to relics of localized dilation. One can thus at best estimate where a hydraulic breakthrough of a clay smear can occur after a localized dilation, and whether an erosion channel can rise along a dilated fault zone up to an outcrop. The probability of such events can hardly be judged because of their wild randomness (cf. Mandelbrot and Taleb [18]).

4 Normal faults and clay smears

Lehner and Pilaar [15] investigated clay smears, in order to judge hydrocarbon seals, by means of lignite mining outcrops west of Cologne. In our earlier paper [5] we proposed other mechanisms than these authors by means of numerical simulations. Before turning to the same region, we consider simpler cases of normal faulting in order to judge sandbox tests and numerical simulations. On this base, scale-independent features of faults and clay smears are identified in the sequel which help to explain hydraulic breakthroughs in the following sections.

Simulations with hypoplastic relations including polar terms (Sect. 2) were validated by sandbox tests with a movable base plate or wall for which shear bands were localized with X-rays [4]. The rather uniform *shear band pattern* of Fig. 2 was obtained with initially dense sand and boundary conditions which represent a uniform stretching. A comparable pattern was obtained in an uncommon sandbox test [27] with a base stretched by means of a spreading grid with hinges under a rubber membrane (Fig. 7). Instead of lateral boundaries for an endless strip as in Fig. 2 the sand layer had lateral slopes. Nevertheless the shear bands (three of them marked by dashed lines in Fig. 7) have nearly the same inclination as in Fig. 2 except near the slopes. Waves in marker bands of Fig. 7 indicate offsets, but differently from Fig. 2 the free surface got wavy towards one side and secondary shear band patterns did not arise. The lack of symmetry can be attributed to the one of the base device, and its section-wise extension was not uniform enough for getting secondary shear bands.

Fig. 6 Sample of gravel with an embedded inclined clay disc, taken from an open-cast mine and re-compressed after remoulding, enclosed by a membrane with 80 cm diameter, after axial loading via smooth end plates with central drainage holes, with confining pressure and hydraulic gradients as under the open-cast mine referred to in Sect. 5

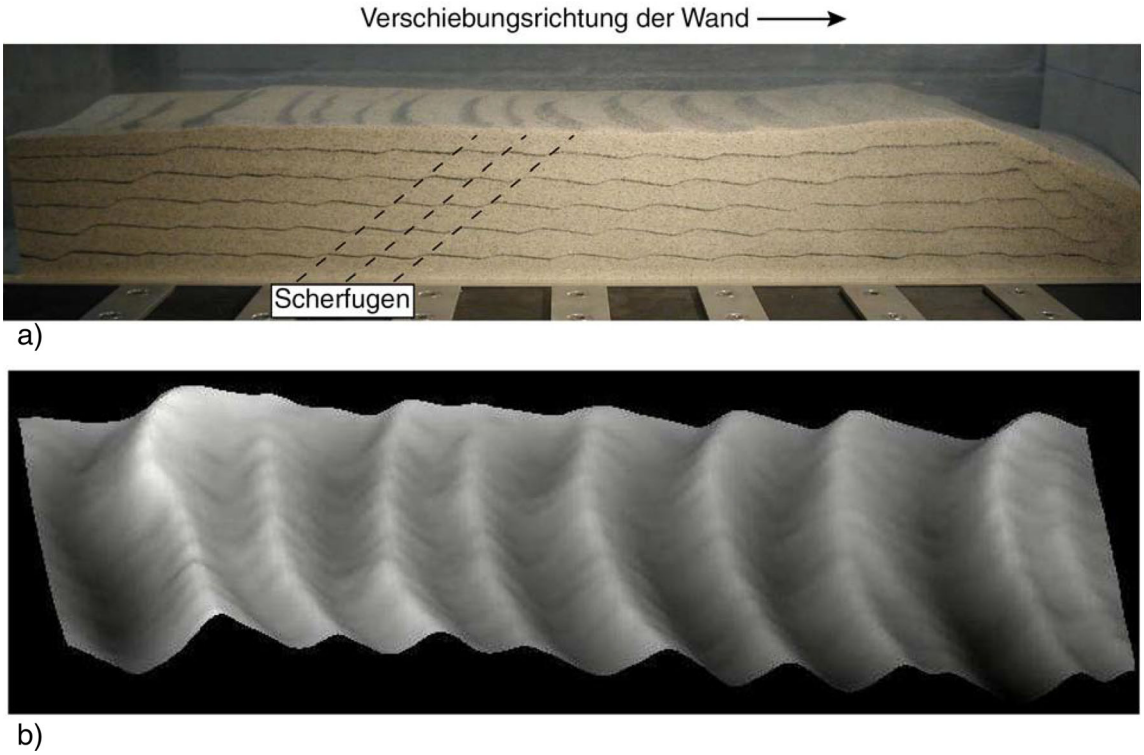

Fig. 7 Shear bands (above, after wetting and cutting) and surface waves (below) by stretching of a sand layer to the right [27])

Sandbox tests are usually carried out with partly displaced bases and walls, and the Mohr–Coulomb rule (Sect. 2) is employed for inferring directions of principal stress from the orientations of shear bands (e.g. Mandl [19]). At least in the case of plane-parallelity such experiments could be replaced by numerical simulations with hypoplastic relations and polar quantities (Sect. 2). This would enable a variation of initial state fields and of boundary conditions beyond imposed displacements. As with Fig. 2 the localized quasi-static dilation in shear band patterns ends due to a contractant collapse which is seismogenic. Arising shear bands are generally aligned with the simultaneos major principal stress, as visible e.g. in Figs. 2 and 7. This correlation gets lost with a contractant collapse, and likewise with further rearrangements of the grain fabric in the stable range (Sect. 2).

The formation of shear band patterns in geological sand layers cannot be simulated with polar quantities as these would require too many finite elements with five grains thickness. A counterpart of Fig. 2 was generated for a layer of geological size with antimeteric lateral boundary conditions, but without polar terms, Fig. 8. The shear bands after 10% extension have nearly the same inclinations as with polar terms, and there are similar secondary patterns and surface wrinkles in both cases. The shear bands after 20% extension are markedly flatter without polar terms, while the free surface exhibits offsets only with them. The average major principal stress σ_1 remains vertical, so the Mohr–Coulomb relation for the shear band direction relative to σ_1 gets lost with further displacements after a dilatant localization. As this relation holds true for a wide range of finite element and layer sizes it may be considered as a *scale-independent* feature of slow tectonics. However, sizes of grains and clay layers influence distances and widths of faults in a way which cannot be clarified only with sandbox tests and finite element simulations.

Figure 9a is a geological cross section of the Lower Rhenish sediment basin west of Cologne. Profiles from numerous boreholes down to the rock base were interpolated by means of sediment layers. A half-graben appears right of the deepest point with *normal faults*, whereas the left half exhibits a more complex tectonic pattern which may be attributed to a combination of extension and strike-slip motion of the rock base. Evidently a depression was formed by a tectonic extension and filled by sediments. Offsets in the investigated part of the rock base indicate deeper faults, but do not enable a unique continuation of them down to the magma base. It appears that deep-seated strike-slip motions produced a wrench faulting with steep and inter-twining faults [20] in addition to normal faults.

The half-graben from the profile without exaggerated heights (Fig. 9b) was simplified for our simulation with a hypoplastic relation, Fig. 9c. A bell-shaped depression was laterally extended and loaded simultaneously by a bell-

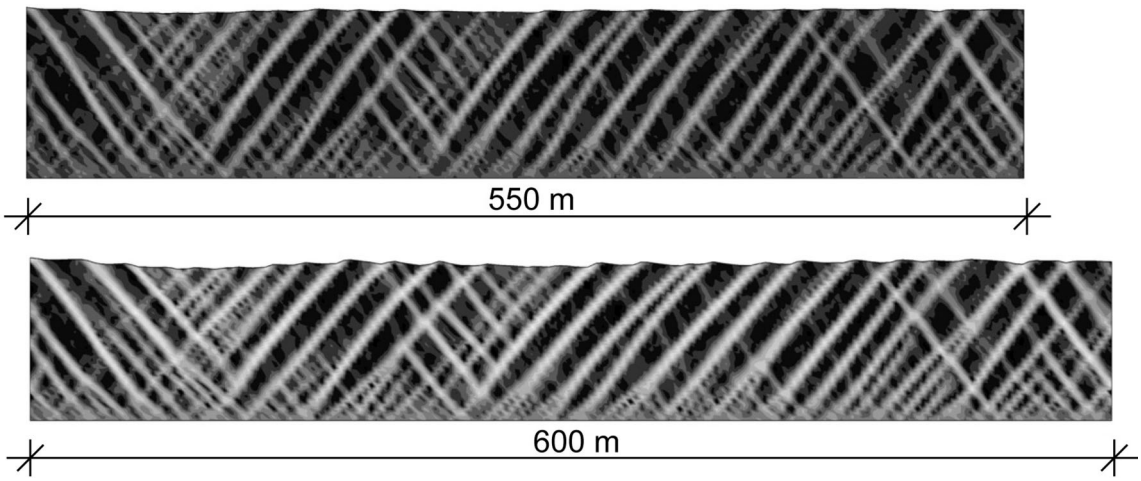

Fig. 8 Simulated shear band patterns of an initially dense and 500 m wide sand layer [5]

shaped surface pressure (not drawn in the figure). With this substitute of a synsedimentary extension the deformed finite element mesh exhibits synthetic normal faults near the point of deflection of the depression, and antithetic ones in addition more outside and inside. The synthetic faults resemble the real ones in Fig. 9b, whereas antithetic ones are less marked in situ and not noted in the profile inferred from boreholes. As outlined further above the artificial faults are as wide as the finite elements and arise by dilation, so only their orientation versus the major principal stress is scale independent.

As any sediment basin the Lower Rhenish one west of Cologne evolved alongside with a depression due to a tectonic extension, which was accompanied by a deep-seated strike-slip motion as a growing gap between tectonic plates is not straight and has ends. This leads to synthetic and antithetic faults, partly steeper wrench faults elsewhere, and/or an inseparable combination of them. As outlined above shear bands in sandbox tests can indicate stress alignments, while numerical simulations can indicate stress fields plus shear band directions. Both methods employ rather arbitrary boundaries and conditions for them. Numerical simulations are not strictly legitimate for geomechanical critical phenomena as spatial and temporal derivatives are no more justified (Sect. 2), and the upscaling of sandbox test results is likewise questionable. However, three *scale-independent features* of geo-matter remain: the Mohr–Coulomb relation of shear band and stress directions, a quasi-static successive localized dilation and kinetic chain reactions thereafter (cf. [9]). The latter matches the moderate seismic activity of rock under the Lower Rhenish sediment basin, which suits also to the high packing density of granular formations inferred from the resistance to penetration probing.

Clay smears, which have first been investigated in outcrops of the Lower Rhenish sediment basin [15], indicate normal faults as offsets of clay layers like in any sediment basin. Their shape is empirically determined by the ratio s/d of fault offset s and clay layer thickness d, [26]. For s/d below ca. 8 typical clay smears have roughly S-shaped boundaries along the transition between opposite source layers, and an inner part of thickness ca. $d/6$ parallel to the fault. This shape was likewise obtained in a numerical simulation with a clay layer between sand layers upon a base which is shifted like a rock base with a normal fault (Fig. 10) [5]. The initially dense sand (modelled as hypoplastic, Sect. 2) dilates within the widening fault zone, while the clay (modelled as visco-hypoplastic) is sheared into the growing clay smear without volume change. Thus the balance of clay mass is satisfied during the simultaneous growth of s and d with an asymptotic clay smear thickness of ca. $d/6$. This mechanism works without an extrusion from the source layer towards the fault as proposed by Lehner and Pilaar [15], which is also questionable as the gradient of pressure from the surroundings towards the fault is too low.

Lehner and Pilaar's [15] paradigmatic clay smear (reprinted in the overview by Vrolijk [26] exhibits *shear bands* in sand and clay which do not appear in our simulation. Shear bands could at best be reproduced qualitatively for the dilated sand in the fault by means of a finer element mesh (cf. Fig. 8), but not in detail as the resolution required for polar quantities (cf. Fig. 2) is not feasible for a fault with sand and clay. The shearing resistance of the clay grows substantially by rapid shearing as during earthquakes, this can cause a kind of cavitation due to negative pore water pressure (Sect. 2). This means a localized dilation of clay which eludes as yet any calculation. The clay contracted again during the far longer aseismic

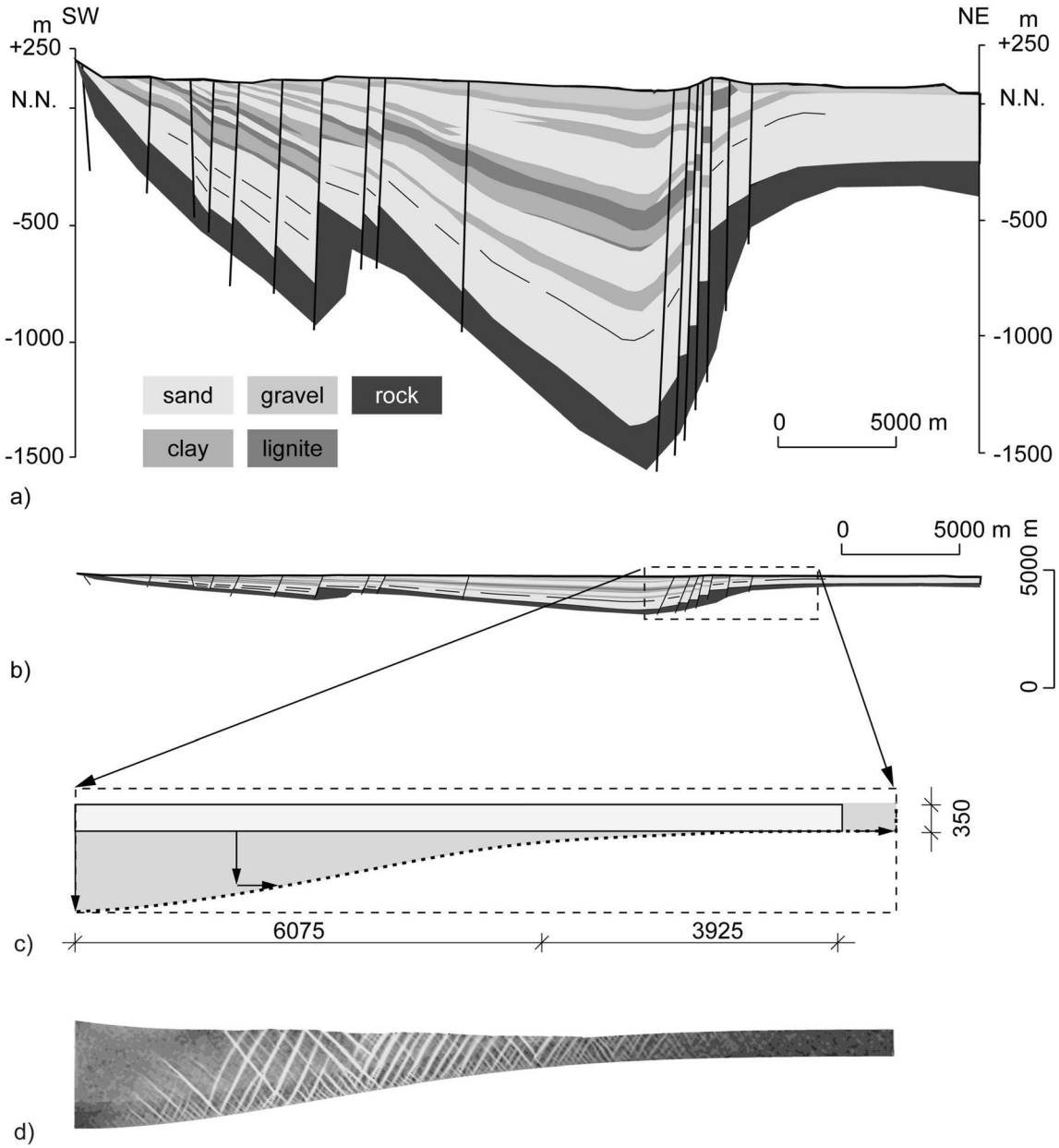

Fig. 9 Cross sections of the Lower Rhenish basin: **a** interpolation from borehole profiles with exaggerated heights, **b** same without exaggeration, **c** simplified cross section of a NE part with imposed stretching and depression (opposite heap for sedimentation not shown), **d** pattern of dilated faults obtained by numerical simulation [5]

intervals assumed for our simulation. The latter is legitimate for the stable range up to its rim with a critical stress ratio ($\tau/p' = \tan\varphi_c$), but not beyond with critical phenomena.

As outlined by Knufinke [13], and more in detail by Lehner and Pilaar [15], several clay smears observed in mining outcrops west of Cologne were not sigmoid, but exhibited *gaps* so that they could not work as seepage barriers. Vrolijk [26] links such cases with a ratio *s*/*d* of fault offset and source layer thickness beyond ca. 8, but point out that gaps occur occasionally also below this threshold. This suits to the wild randomness of critical phenomena in general, and in particular of the ones with geo-matter. This kind of randomness is typical not only for earthquakes [8], but also for gaps in clay smears. Therefore observations of offsets and clay layers are indispensable for judging the competence of clay smears, but even so gaps cannot be completely excluded. A competent major hydraulic seal for a lignite mine is described in the sequel, but a judgment only by means of water levels and pumping rates of wells does not suffice for the specification of weak points in clay smears [26].

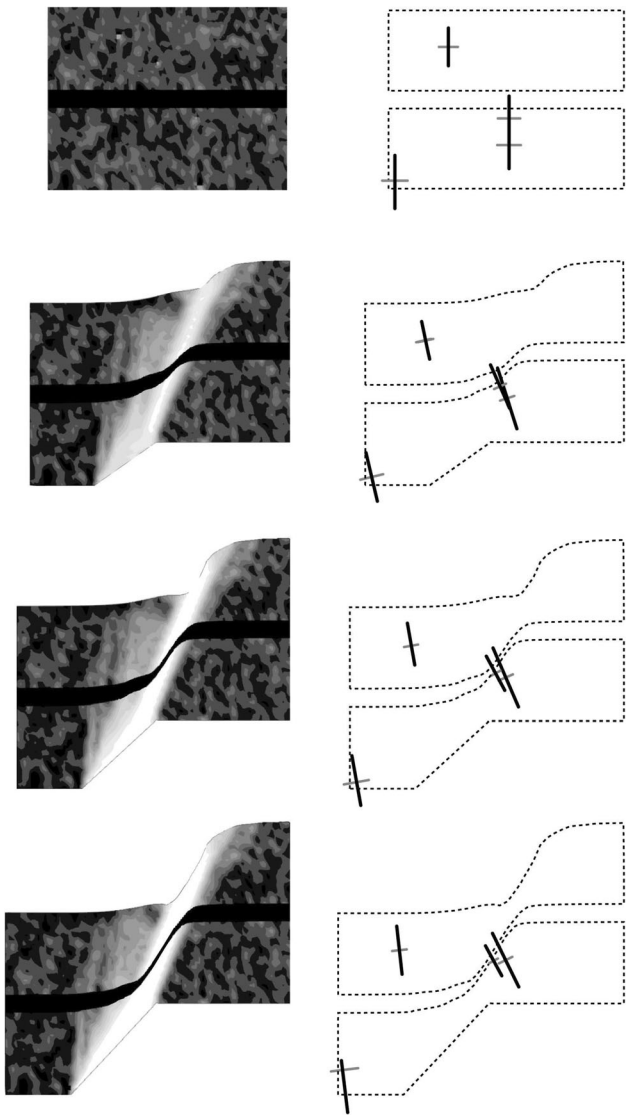

Fig. 10 Simulated evolution of a clay smear. Left: clay black, dense sand gray, dilated sand white; right: crosses represent principal stresses [5]

5 Evaluation of an event in a lignite mine

About 25 years ago turbid water accumulated in a 350 m deep lignite mine west of Cologne [25]. The flow dwindled after pumping out groundwater from wells of ca. 400 m depth, and came to an end after some days. For enabling the excavation the groundwater table had been lowered by ca. 400 m from the far-field level a few meters under the natural surface. Geodetic measurements indicated horizontal displacements towards the growing excavation of up to ca. 0.4 m, and a pit bottom settlement of up to ca. 0.1 m during the outflow.

A cross section, based on ca. 700 m deep boreholes, exhibits dominant layers of sand and thinner ones of clay (Fig. 11). Offsets indicate a major normal fault and two minor ones with inclinations as in Fig. 9. The thickest clay layer with clay smears about 100 m under the pit worked as seal for the reduced ground water pressure against its far-field level. A *breakthrough of a clay smear* occurred where its critical hydraulic gradient was reduced to the actual one. This led to an internal erosion up to an outflow in the pit and came to an end after pumping out water. This mechanism is considered now in detail.

The cross section of Fig. 11 was translated into a two-dimensional *finite element mesh* with finer resolution near the excavation and along faults. The mechanical behavior of sand and clay was modelled by elasto-hypoplastic and visco-hypoplastic relations, respectively, material parameters were determined by means of triaxial tests (Sect. 2). The initial void ratios of sand were adapted to the depth-dependent effective pressure p' and to the densification by repeated earthquakes, which is confirmed by penetration probing. The initial void ratios of clay were adapted to the p'-values before the excavation and to the geological resting time, and they suit to the ones of excavated layers. Lignite was modelled as a kind of clay with a higher viscosity due to the organic content. The major fault was represented by a strip with a mixture of sand and clay.

An effective stress field prior to groundwater lowering and excavation was generated by imposing the specific weight minus hydraulic uplift gradually. Thus the calculated average ratio of horizontal and vertical effective stress components attained ca. 0.5, while it was somewhat higher in clay and lower in sand layers. The lowering of groundwater from just below the surface to sufficiently below the pit was simulated by switching off the uplift above the major water seal, it produced a hydraulic pressure difference of almost 1.5 MPa at the seal. The calculated surface settlement of ca. 1.3 m due to the reduction of uplift matches field measurements. Thereafter the excavation was simulated by removing finite elements gradually. The resulting horizontal displacements of the slopes were reduced by factors for the three-dimensional excavation and re-deposition, calculated with a simplified mesh. They ranged from ca. 0.1 m below to 0.5 m above along slopes and exceeded the measured ones by factors from ca. 1.2 above to ca. 1.7 below. As these deviations can be attributed to the successive placement of measurement points during the excavation the numerical model was thus validated [12].

At the right-hand side of the cross section, Fig. 11 calculates horizontal displacements are about twice as big as at the left-hand side. Calculated relative displacement paths of opposite points at the major fault due to the excavation are represented in Fig. 12. For the point pair P2-P1 near the pit the path matches observations when taking into account the three-dimensional reduction and the delayed placement of measurement points. The deeper point pairs P4-P3 and

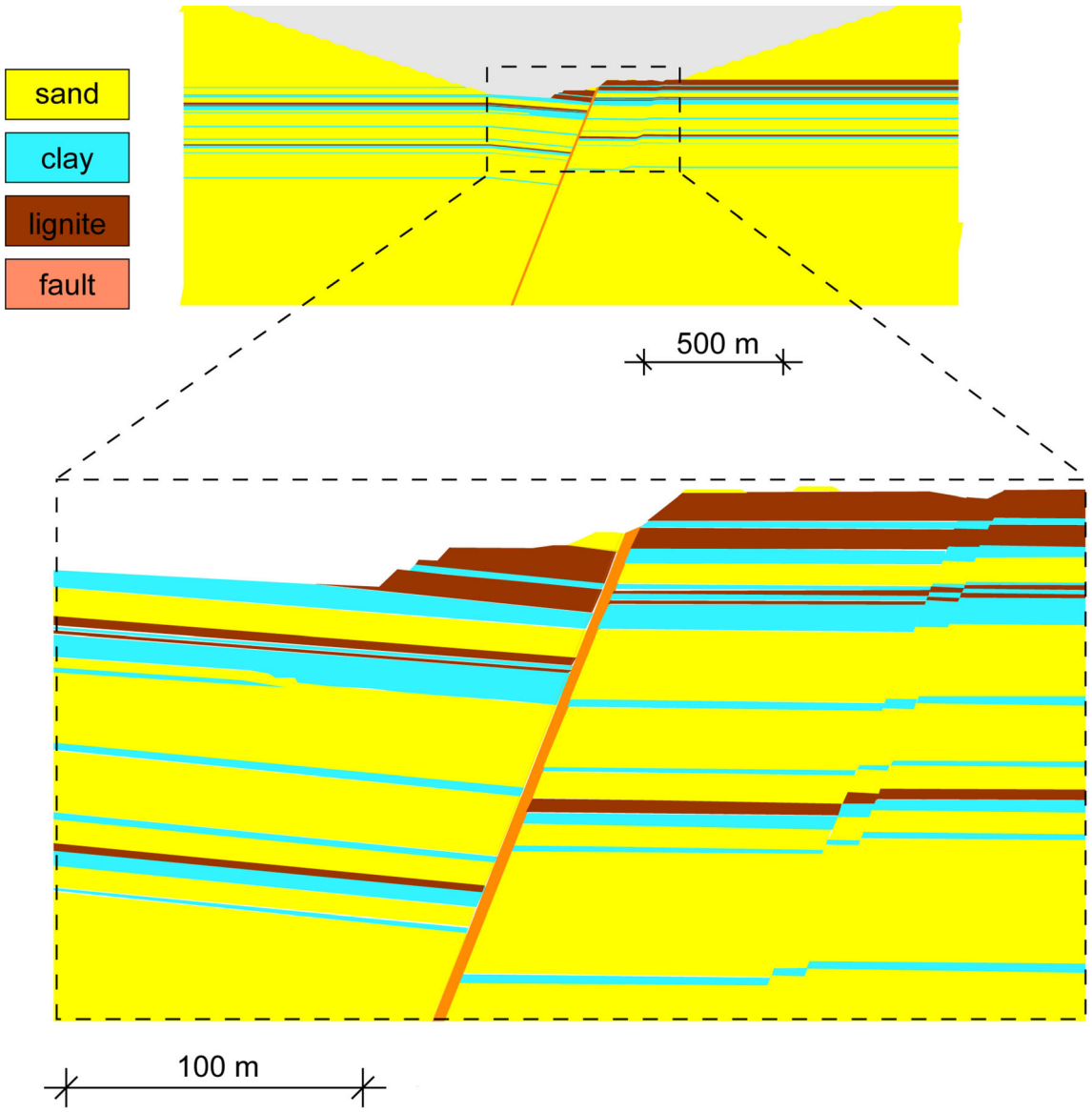

Fig. 11 SW-NE cross section of an open-pit mine in the Lower Rhenish basin at the site with an outflow, viewed from SE towards the end of a trench

P6-P5 indicate likewise a *reversed shearing*, compared with the previous tectonic one, which is accompanied by a dilation due to pressure reduction and shearing (cf. Sect. 2). A three-dimensional simulation (Fig. 13) shows that the excavation-induced deformation of an idealized clay smear is maximal under the corner of a trench.

The reversed shearing in the major fault had a far higher rate than before by tectonic stretching, this rise led to a localized dilatation where the deformation sufficed to reach a critical point (cf. Sect. 2). The seepage force due to the hydraulic height difference could thus lead to an *erosion of fines* from dilated shear bands in a clay smear towards a neighbored grain fabric. According to Fig. 5 critical gradients, i.e. those which suffice for the onset of erosion, would range from about 5000 to 2000 for an effective pressure $p' = 0.4$ MPa and adjacent pore openings from 0.5 to 1.5 mm, whereas they would be about ten times bigger without a previous shear localization (cf. Sect. 2).

For a transfer of these lab results to the outflow in the lignite pit *spatial fluctuations* and *viscous effects* have to be taken into account. The major water seal about 100 m under the pit is rather a composite of clay and sand. Therein a uniform clay layer of 3.5 m thickness—taken from borehole profiles—would be thinned to a clay smear of $d_c \approx 3.5/6 \approx 0.6$ m thickness (cf. Sect. 4), so the water pressure difference $\Delta p_w \approx 1.5$ MPa named above would cause a hydraulic gradient $\Delta p_w/\gamma_w d_c \approx 250$ with $\gamma_w \approx 10$ kN/m^3. This is at most an eighth of the critical gradient by

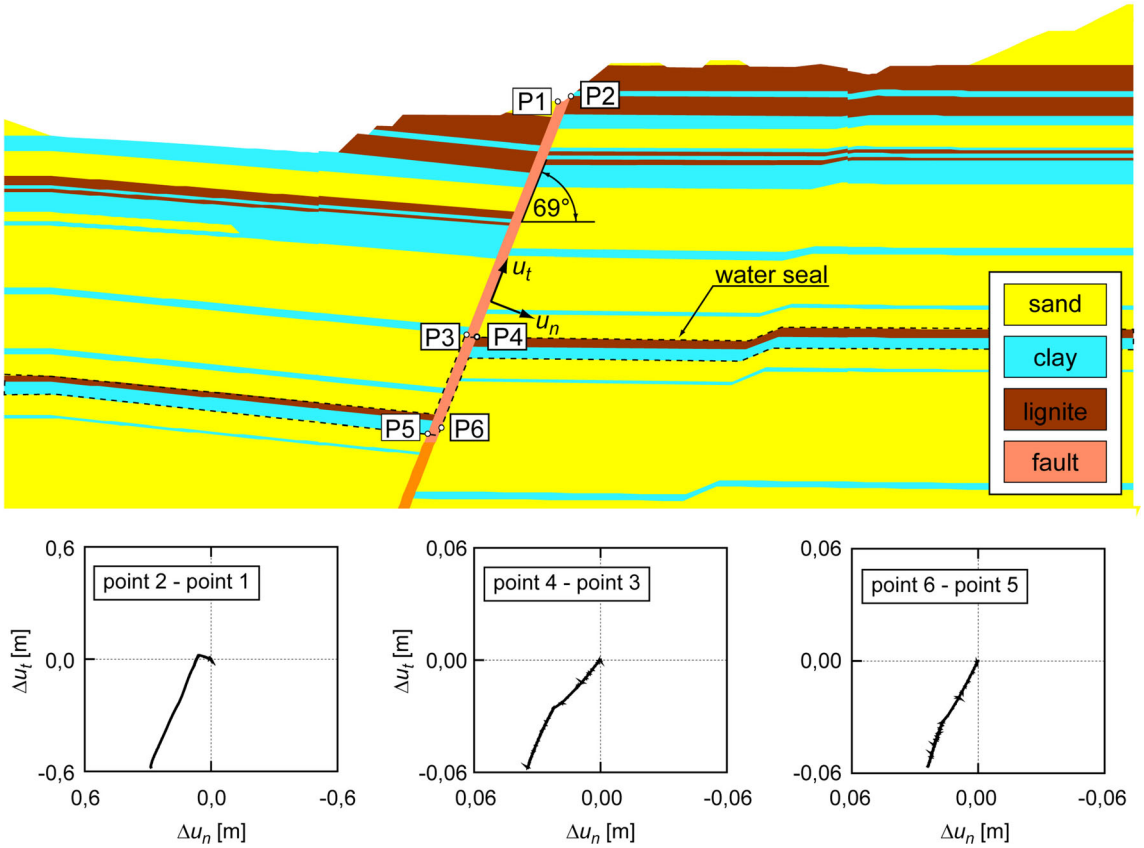

Fig. 12 Calculated relative displacement paths for pairs of points at the major fault of Fig. 11. Dilation and backward shearing negative

Fig. 5 for $p' = 0.4$ MPa with shear bands and a neighbored pore width of 1.5 mm. So how could water break through a clay smear?

As outlined in Sect. 4 clay smears are warped irregularly by critical phenomena so that they can get thinner than 1/6 of the source layer thickness. The reversed shearing—almost without seepage in clay because of the high rate—due to the excavation caused first a reduction of p' and τ in clay smears (cf. Sect. 2). Its continuation, as before with about ten million times higher rate than the previous tectonic shearing, could lead to a critical point with a much higher p' and τ. The rather big deformation under the corner of the trench (cf. Fig. 13) caused a deformation with localized dilatation and shear softening, in particular at the interface of a clay smear with a coarse-grained formation, so that the critical hydraulic gradient got smaller. It could thus reach the actual gradient, which fluctuates due to variations of the clay smear thickness (cf. Sect. 4), so that an erosion set on.

The hydraulic breakthrough and the subsequent evolution of an erosion channel followed as a *chain reaction* which eludes as yet mathematical treatment. The hydraulic gradient in the clay smear increased with the opening so that the erosion therein accelerated. The resulting upwards seepage followed the fault as therein the sand was dilated. The ensued hydraulic gradients, although being far lower than initially in the clay smear, sufficed for an erosion of dilated sand (cf. Sect. 3) so that a channel could attain the pit. The outflow appeared about 20 m south-eastwards of the outcrop of a major fault, apparently a minor antithetic fault (cf. [21]) was dilated by the excavation-induced unloading and shearing so that it deviated the rising erosion channel. Thus water with traces of H_2S rose from under the weakened clay seal. The outflow came to an end when the water pressure under the clay smear got lower by pumping from wells near the pit. As the water pressure difference Δp_w did not disappear completely the end of flow indicates a *self-healing* of the clay smear like in the triaxial test of Fig. 6: the bottom of the pit settled by about 0.1 m during the flow, thus erosion channels were closed when the major fault was sheared again in the natural direction.

The further progress of the excavation did not reach the next major fault (cf. Fig. 9) so that no further outflow could occur. Thereafter the open-cast mining was carried out with another direction of the trench so that the orientation of the excavated slope deviated markedly from the SE-NW direction of the major faults. Thus the reversed shearing of clay smears by the excavation was substantially reduced so

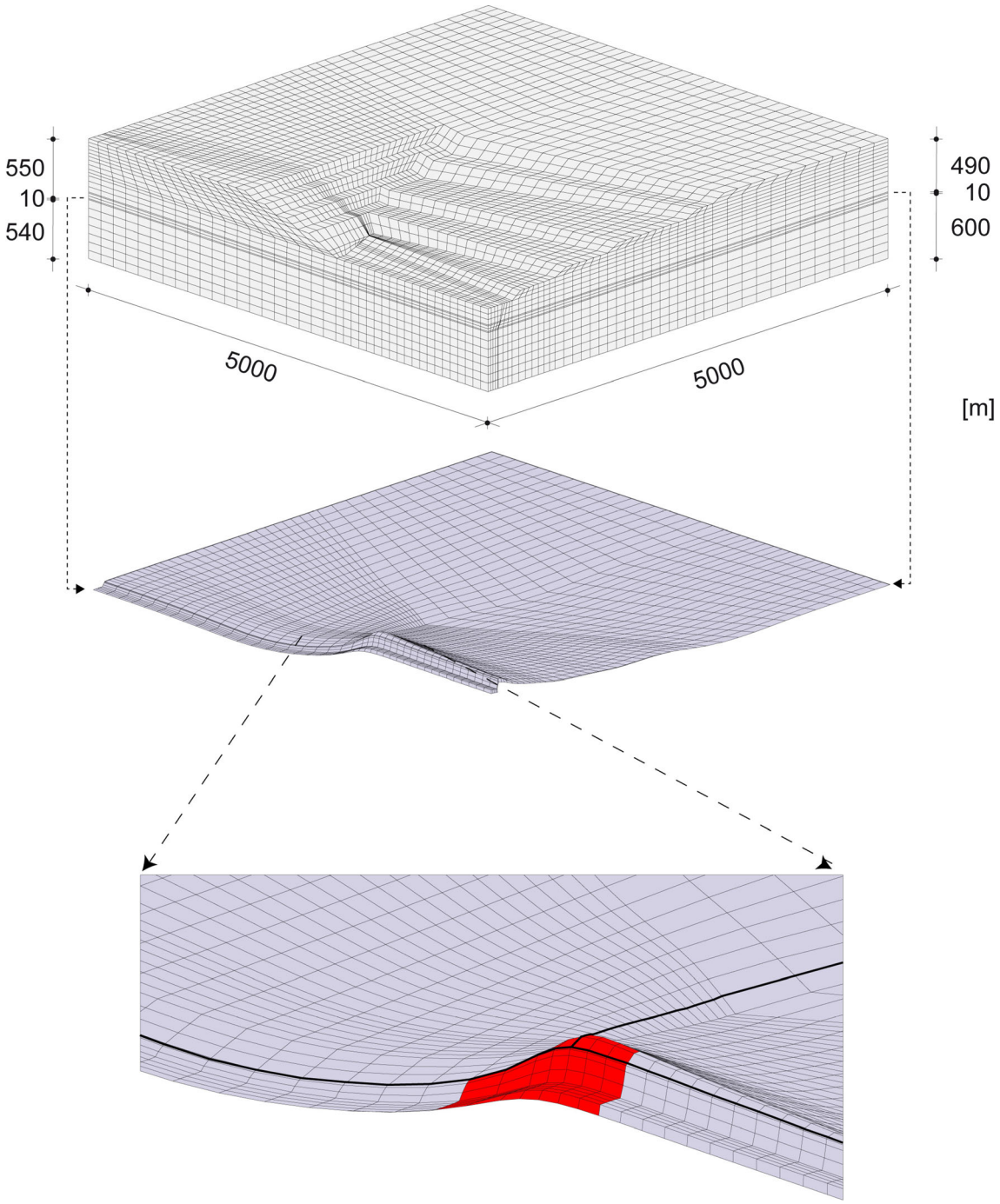

Fig. 13 Simulated excavation of a trench with a simplified clay layer and smear. Above: one half of the finite element mesh (viewed towards the end of the trench), below: clay layer and smear (deformation exaggerated), further below: blown-up detail (part with maximal deformation marked)

that hydraulic gradients could no more get critical. Outflows due to hydraulic breakthroughs of clay smears did not occur ever since in lignite mines of the same company.

6 Natural hydraulic breakthroughs

Hydraulic breakthroughs of clay smears damaged by natural actions differ from the ones by open-cast mining in some aspects, but there are common features. Natural cold eruptions occur more often and in wider regions, and produce dominantly mud and gas. They arise in about ten

times bigger depths where pressures are higher and void ratios lower, but with similar faults and clay smears. An erosion sets on when and where the hydraulic gradient reaches the critical one. Such critical phenomena are induced by synseismic deformations after the accumulation of methane under a hydrocarbon seal. Let us consider mechanisms now in detail.

Normal and wrench faults have outcrops where eruptions can arise. *Mud volcanoes* emit also methane and are driven by the same. Naylor [20] refers to wrench faults near the north coast of Venezuela, that's where Humboldt found volcanitos at outcrops of faults (described in his 'Kosmos'). Bigger mud volcanoes occur along the western coast of Pakistan with strike-strip faulting due to accretion [3]. Gas rising offshore liquefies sediments and reaches the surface as bubbles, and mud is carried away by currents. This was observed likewise along the Corinthian gulf during the Aegion M 7 earthquake 1995: near the south coast rising hot gas drove out fish, farther west shallow sea bottom turned into a suspension which was washed out by tidal currents so that craters were left back. The region had evolved by normal and wrench faulting alongside with sedimentation of sand and clay. Not only in these cases clay smears act as parts of a seal for methane and water, which can break by earthquakes and get eroded so that mud and methane rise in faults.

Natural methane arises by anaerobic degradation of plankton relics in marine sediments. These pile up to a sandwich in basins which get deeper by tectonic extension. The latter leads to faults up to the surface, which can be more complex than outlined in Sect. 4 due to surface erosion. The effective pressure p' of gas-bearing formations, typically around 50 MPa in ca. 3 km depth, causes lower void ratios than at water seals under lignite mines, but fault systems are similar. Methane is trapped by intact clay layers and clay smears if it cannot evade sidewards. Leaving aside diapirs as faults thereby hardly reach the surface [19], methane-trapping seals have complex three-dimensional shapes which elude numerical simulations until present (Sect. 4).

Trapped gas attains an *excess pressure* when it is further generated and no more dissolved in pore water. It cannot reach a cap-like seal as pore water in between likewise cannot evade. Thus the water pressure p_w gets higher than just above the seal so that this experiences an increasing gradient of p_w. This is higher in clay smears than in their source layers so that the seal breaks first in faults when the critical hydraulic gradient drops to the actual one. Clay smears can break by extremely fast deformations during earthquakes as then the highly compressed clay is no more plastic, but cataclastic so that shear bands and cracks arise (Sect. 2). Thereafter the seepage force due to pressurized enclosed gas can cause an erosion into dilated granular formations above clay smears in faults (cf. Sect. 4). Mud and gas can thus rise in erosion channels evolving in major faults up to a cold eruption at outcrops.

We do not take over the usual assumption that gas breaks through a seal after a capillary entry. Mud can be produced from highly compressed clay only by erosion with water from below, where the latter was trapped by the seal alongside with gas producing an excess pressure. Differently from open-cast mining, clay smears can break in wide zones due to synseismic shearing, and a self-healing is no more possible after a major erosive loss of clay. Therefore natural breakouts are more widespread and more erratic than technogenic ones. As outlined in Sect. 5 outflows of water in open-cast mines can be avoided, whereas natural cold eruptions occur with a wild randomness—characteristic of critical phenomena with geo-matter in general (Sects. 2 and 4)—which eludes prediction and control. Eruptions of gas and mud—sometimes also near production boreholes, resulting likewise from a progressive erosion of damaged clay seals—come to an end by the exhaustion of gas inclusions with excess pressure.

Turning again to Delisle's [3] paper on mud volcanoes in Pakistan, we think that our mechanisms enable a more consistent explanation. We cannot follow his hypothesis of under-compacted clay millions of years after the sedimentation (cf. Sect. 4). Without internal erosion clay—compressed according to overburden and resting time (cf. Sect. 2)—cannot turn into mud, this requires a damaged clay seal and water with excess pressure from below. We specify Delisle's 'destabilization' as a succession of critical phenomena (cf. Sect. 4), taking over the gas-driven rise of mud in faults without assuming open fractures. Cracks in sediments–including faults–are almost totally closed by the overburden pressure, but can be widened by rapid shearing and and high hydraulic gradients, whereas Delisle [3] refers to an extrusion of mud along cracks. We attribute the continued emission of gas and mud, reported e.g. for some sites of Pakistan by this author, to a never-ending succession of critical phenomena.

Such events exhibit a *wild randomness* in Mandelbrot's [17] sense, not a mild one for which mean-field theories would suffice. Mandelbrot and Taleb [18] explain the difference with 10.000 persons in a stadion: if one person enters average biological properties remain almost the same, but the fortune per capita rises substantially if the one is Bill Gates. In other words, power law distributions replace normal distributions if one extreme event matters as much as all the 'normal' ones together. An example with geo-matter is the Gutenberg-Richter relation for the number N of earthquakes with released energy E or more, viz.

$N = N_r(E/E_r)^{-b}$ for $E \geq E_r$, $N = 0$ for $E < E_r$ and $E > E_m$

with an exponent $b \approx 1$, an upper cutoff E_m, a lower one E_r and a total number N_r of events. With it the probability N/N_r of events with E or more, triggered by a seismic background noise with average energy E_r, is $P \approx E_r/E$ with $E_r \leq E \leq E_m$. This power law is an approximation of a stable Levy distribution, which is obtained if P does not depend on its previous values [8]. Stability in this context means that any weighted superposition of events leads to the same cumulative probability distribution. The exponent $b = 1$ is justified if the response of the lithosphere to a magma drive is rate-independent (cf. Sect. 2), then the number N of events is proportional to the magma shift. An upper cutoff E_m is needed as otherwise expected value and variance of E diverge.

The Gutenberg-Richter relation with $b \approx 1$ is empirically validated, but its cutoffs needed for a probabilistic evaluation are not easily determinable. To begin with, the released energy E can at best be crudely estimated from seismograms and tectonic displacements. The upper bound E_m, increasing with the size and activity of a seismically active region, requires a tectonic extrapolation. The lower bound E_r, which serves also as a reference value for scaling E, can hardly be identified from a background noise. Despite this indeterminacy the empirically and mathematically justified power law is of use as it is a feature of critical phenomena in general (cf. [21]). As outlined in the previous sections critical phenomena with geo-matter are either quasistatic with successive formation of shear band or crack patterns, or kinetic with chain reactions (cf. [9]). Both exhibit scale-independent features with spatio-temporal fractality, therefore lab tests are instructive despite strong fluctuations. The fractality eludes a mathematical treatment of geo-mechanical critical phenomena with continuum models, these can at best work up to the verge of stability (cf. Sect. 4).

Natural hydraulic breakthroughs of clay smears can arise from successive critical phenomena alongside with methane-generating sediments. As long as the reaction of the lithosphere is nearly rate-independent, so that $b \approx 1$ holds for successive events with a wild randomness, their combined probability obeys the same power law. This indicates scale-independent features as the ones proposed further above, although the low number of data from natural cold eruptions eludes a statistical quantification.

7 Conclusions

The eruption of water, mud and gas at the outcrop of faults can be traced back to a breakthrough of clay smears by seepage forces after rapid deformations. Clay smears arise in normal or wrench faults, patterns of which evolve with synsedimentary extension and/or with strike-slip shearing of the rock base. Their average thickness tends to about 1/6 of the one of the source layer, while the thickness of the dilated fault zone grows by about 1/6 of its further offset. With a far more rapid deformation than before shear bands and cracks can arise in clay smears, thus the critical gradient for erosion into granular formations above gets lower. If the critical hydraulic gradient drops to the actual one erosion channels evolve and rise in faults up to a breakout at an outcrop.

An outflow of water occurred in an open-cast mine in the Lower Rhenish sediment basin, and came to an end after pumping out water from neighbored wells. A thorough investigation revealed a mechanism as outlined above with a clay smear ca. 100 m under the end of a trench by a rapid (in a geological time-scale) reversed shearing due to the excavation, and a subsequent self-healing. Finite-element simulations reproduce observed patterns of normal faults and clay smears, and show that deformations which suffice to weaken clay smears could occur under the end of the trench as the excavated slope was nearly parallel to a nearby fault. The succession of seepage and erosion cannot be calculated because of fractal fluctuations. Nevertheless the systematic dependence of the detrimental deformation of a clay smear on the alignment of excavation and fault helped to exclude outflows due to hydraulic breakthroughs ever since.

Natural cold eruptions produce mud and methane, they are widespread and erratic. Natural gas is trapped alongside with water by cap-like three-dimensional combinations of clay layers and clay smears which are highly compressed by the overburden pressure. An excess pressure evolves by the continued bio-degradation of plankton relics so that the hydraulic gradient rises in the clay seal. It can reach a critical amount in clay smears if rapid deformations during earthquakes produce dilated shear bands and cracks. Then erosion sets on towards adjacent granular formations above and proceeds in channels rising in faults, thus mud and natural gas are emitted at or near outcrops until the source of gas with excess pressure is exhausted.

Prediction and control of natural hydraulic breakthroughs are hardly possible because of their wild randomness. Probabilities can at best be judged qualitatively like the ones of earthquakes as far as cap rocks and methane under them are known. We propose partly novel mechanisms for critical phenomena leading to cold eruptions which exhibit wild randomness, but also systematic features.

Acknowledgement This paper is dedicated to the mining engineer Professor Karl Pierschke (1941–2012), who worked for RWE Power and lectured at the Technical University Clausthal/Germany. He realized the relevance of excavation-induced deformations for a water outflow and initiated a thorough investigation.

Funding Open Access funding enabled and organized by Projekt DEAL. Funding and consent for publication by Power AG is gratefully acknowledged. We declare no conflicts of interest.

Data availability No source data and materials can be made available.

Declarations

Conflict of interest The authors declare that they have no conflict of interest.

References

1. Balthasar K, Gudehus G, Külzer M, Libreros-Bertini A-B (2006) Thin layer shearing of a highly plastic clay. Nonlinear Process Geophys 13:671–680
2. Darwin GH (1883) On the horizontal thrust of a mass of sand. Proc Inst Civ Eng LXXL:350–378
3. Delisle G (2004) The mud volcanoes of Pakistan. Environ Geol 46:1024–1029
4. Gudehus G (2011) Physical soil mechanics. Springer, Berlin
5. Gudehus G, Karcher C (2007) Hypoplastic simulation of normal faults without and with clay smears. J Struct Geol 29:530–540
6. Gudehus G, Jiang Y, Liu M (2010) Seismo- and thermodynamics of granular solids. Granul Matter 13(4):319–340
7. Gudehus G, Touplikiotis A (2016) Wave propagation with energy diffusion in a fractal solid and its fractional image. Soil Dyn Earthq Eng 89:38–48
8. Gudehus G, Touplikiotis A (2018) Seismogenic chain reactions and random successions of them. Paper for Soil Dyn Earthq Eng
9. Gudehus G, Lempp C (2022) Tectonic critical phenomena with dilatancy in lithosphere sections. Hallesches Jahrbuch für Geowissenschaften, Band 45, Heft 1, Seite 37–61
10. Jiang Y, Liu M (2009) Granular solid hydrodynamics. Granul Matter 11:139–145
11. Kadanoff LP (1999) Built upon sand: theoretical ideas inspired by the flow of granular materials. Rev Mod Phys 71(1):435–444
12. Karcher C (2003) Tagebaubedingte Deformationen im Lockergestein. PhD thesis, Veröffentl Institut für Bodenmechanik und Felsmechanik, University in Karlsruhe, Heft 160
13. Knufinke H-U, Kothen H (1996) Die Tektonik der Niederrheinischen Bucht vor, während und nach der Hauptflözbildung. Braunkohle Surf Min 49:473–479
14. Kolymbas D (1991) An outline of hypoplasticity. Arch Appl Mech 61:143–151
15. Lehner FK, Pilaar WF (1997) The emplacement of clay smears in synsedimentary normal faults: inferences from field observations near Frechen, Germany. Hydrocarbon Seals, Norwegian Petroleum Society Special Publications No 7, Ed. P. Moeller-Pedersen and A.G. Koestler, pp 39–50
16. Lempp C, Menezes F, Schöner A (2020) Evolution of shear bands and cracks in multi-stage triaxial tests with water-saturated sandstone: a study of micro-tectonics with a fractal perspective. J Struct Geol 138:104092
17. Mandelbrot B (1999) Multifractals and 1/f-noise—wild self-affinity in physics. Springer, New York
18. Mandelbrot B, Taleb N (2006) A focus on the expectations that prove the rule. Financial Times
19. Mandl G (1988) Mechanics of tectonic faulting, models and basic concepts. Elsevier, Amsterdam
20. Naylor MA, Mandl G, Sijpesteijn CHK (1997) Fault geometries of basement-induced wrench faulting under different initial stress states. J Struct Geol 8/7:737–752
21. Neugebauer HJ (2003) Complexity of change and the scale concept in earth system modelling. In: Neugenauer HJ, Simmer C (eds) Dynamics of multiscale earth systems. Springer, Berlin, pp 41–63
22. Niemunis A (1992) A visco-plastic model for clay and its FE-implementation. In: Resultats Recents en Mechanique des Soils et des Roches, pp 151–162, XI Colloque Franco-Polonais, Politechnica Gdanska
23. Nübel K (2002) Experimental and numerical investigation of shear localization in granular material. PhD thesis, Veröffentl Institut für Bodenmechanik und Felsmechanik, University of Karlsruhe, Heft 159
24. Persson BNJ (2000) Sliding friction—physical principles and applications, 2nd edn. Springer, Berlin
25. Spiller M, Forkel C, Köngeter J (2004) Inflow of groundwater into open-cast mine Hambach, Germany. J Hydraul Eng 130(7):608–615
26. Vrolijk PJ, Urai J, Kettermann M (2016) Clay smear: review of mechanisms and applications. J Struct Geol 86:95–152
27. Wolf H, Koenig D, Triantafyllidis T (2003) Examination of shear band formation in granular material. J Struct Geol 25:1229–1240
28. Zou Y (2000) Der vom Spannungszustand und Bodengefüge abhängige Erosionsdurchbruch bindiger Böden. Wasserwirtschaft 90(11):554–559